

Comparison of visual servoing approaches on straight lines

Derrar Yasser
Team AutoMed
laboratory d'Automatic de Tlemcen
University of Tlemcen
Chetouane, Tlemcen 13000
Email : derrar.yasser@gmail.com

Malti Abed
Team AutoMed
laboratory of Automatic of Tlemcen
University of Tlemcen
Chetouane, Tlemcen 13000
Email : abed.malti@gmail.com

Résumé—in this paper ,we compare three approaches of visual servoing on four lines .we present in detail the obtaining of the interaction matrix expression for a line. The visual setting consists of the orientation of the projected line in the image space as well as its orthogonal distance compared with the origin of the coordinate system centered in the image space. The three compared approaches consist on the instantiation of the interaction matrix at the current point, the reference point as well as the interaction matrix which is the center of the first two interactions matrix. The results we have obtained show that the use of the latter approach is more adequate to converge towards the reference state.

I. INTRODUCTION

Visual servoing techniques consist in controlling the movements of a dynamic system from information provided by a vision sensor (cameras). Many studies have been undertaken in this field for several years[1]. In fact, it is constantly boosted by new possibilities in terms of computing power, performance of imagers or new robotic applications. Nevertheless, a number of substantive issues are generic to the discipline and can be dealt with independently of any practical considerations. Two main aspects have a great impact on the behavior of any visual servoing scheme : the selection of the visual features used as input of the control law and the form of the control scheme. As for the visual features, they can be selected in the image space (point coordinates, parameters representing straight lines or ellipses,[5], [9], [3], [6], [1]),in the Cartesian space (pose, coordinates of 3D points [14], [15]),or composed of a mixture of both kinds of features attempting to incorporate the advantages of both image-based and position based methods [13], [7], [2]. As for the choice of the control law [5], [12], [2],it affects the behavior of the selected visual features (local or global exponential decrease, second order minimization, ...) and may lead, or not, to local

minima and singularities [3]. In this paper we study and compare three approaches of visual servoing on straight lines.

A. Visual servoing on a straight line :

the principle of our study is visualized a straight line in space.

what is a straight line in space ?

A straight line in the image can be seen as an infinite segment of length and whose center of gravity belongs to the straight line (see Figure1). Using the representation that defines the configuration of the straight line by : (ρ, Θ) .

a straight line is the intersection between two plans in space.

h1 is the first plan and h2 is the second plan.

$$H(X, P_0) = \begin{cases} h_1 = A_1X + B_1Y + C_1Z + D_1 \\ h_2 = A_2X + B_2Y + C_2Z + D_2 \end{cases} \quad (1)$$

A, B, C and D are the parameters of the plan and the intersection between these two plans gives us the following equation :

$$\frac{1}{Z} = \mu(x, P_0) \quad (2)$$

$$\frac{1}{Z} = Ax + By + C \quad (3)$$

we will take a special case when a plan goes through the origin so :

$$D_1 = 0$$

then the equation of the first plane h1 becomes :

$$H(X, P_0) = \begin{cases} h_1 = A_1X + B_1Y + C_1Z \\ h_2 = A_2X + B_2Y + C_2Z + D_2 \end{cases} \quad (4)$$

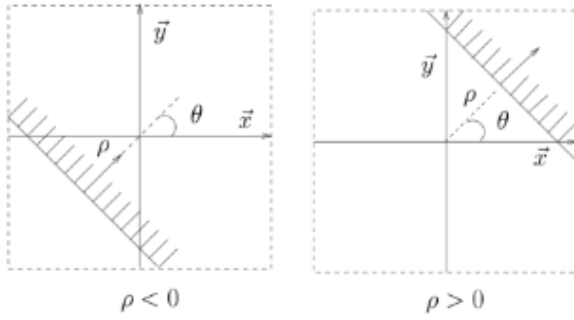


FIGURE 1. représentation (ρ, Θ) des droites

the equation of a straight line in a 2D image is given by the following equation :

$$Ax + By + C = 0 \quad (5)$$

we will represent our equation by the parameters : ρ, Θ ,

$$g(x, p_i) = x \cos \Theta + y \sin \Theta - \rho \quad (6)$$

$$\Theta = \arctan(B/A)$$

$$\rho = \frac{C}{\sqrt{A^2 + B^2}}$$

$g(x, p_i)$ it's primitive 2D

p_i parameterization on function (ρ, Θ)

$$\dot{g}(x, p_i) = 0 \quad (7)$$

$$\dot{g}(x, p_i) = 0 \quad (8)$$

$$\frac{\partial g}{\partial x}(x, p_i) + \frac{\partial g}{\partial p_i}(x, p_i) = 0 \quad (9)$$

$$\dot{\rho} + (x \sin \Theta - y \cos \Theta) + \dot{x} \cos \Theta + \dot{y} \sin \Theta = 0 \quad (10)$$

$$x = f(y, \rho, \Theta)$$

$$x = \frac{\rho}{\cos \Theta} - y \tan \Theta \quad (11)$$

$$A = -x \dot{\Theta} \sin \Theta + y \dot{\Theta} \cos \Theta - \dot{\rho} \quad (12)$$

$$= -\left(\frac{\rho}{\cos \theta} - y \tan \theta\right) \sin \theta + y \dot{\Theta} \cos \theta - \dot{\rho} \quad (13)$$

$$= y \dot{\Theta} \tan \Theta + \cos \Theta + \tan \Theta \rho \dot{\Theta} - \dot{\rho} \quad (14)$$

$$= \left(\frac{\Theta}{\cos \Theta} y - (\dot{\rho} + \rho \dot{\Theta} \tan(\Theta))\right) \quad (15)$$

avec

$$\begin{pmatrix} \dot{x} \\ \dot{y} \end{pmatrix} \in D \quad (26)$$

the interaction matrix of a point in the case of a point of coordinates $x = (x, y)$ in the image space and of depth Z in the reference of the camera, the interaction matrix is given by :

$$\begin{pmatrix} \dot{x} \\ \dot{y} \end{pmatrix} = \begin{bmatrix} \frac{1}{Z} & 0 & \frac{-y}{Z} & -xy & 1+x^2 & -y \\ 0 & \frac{1}{Z} & \frac{-x}{Z} & -(1+y^2) & xy & x \end{bmatrix} * v \quad (16)$$

avec v it's speed

$$v = [v_x, v_y, v_z, \omega_x, \omega_y, \omega_z]'$$

$$-\frac{\dot{\Theta}}{\cos \Theta} y + \dot{\rho} + \rho \tan \Theta \dot{\Theta} = y K_1(p_i, p_0) v + k_2(p_i, p_0) * v \quad (17)$$

$$x \dot{\Theta} \sin \Theta + y \dot{\Theta} \cos \Theta - \dot{\rho} = -\left(\frac{\rho}{\cos \Theta} - y \tan \Theta\right) \quad (18)$$

$$\begin{pmatrix} K_1 \\ k_2 \end{pmatrix} = \begin{bmatrix} -\lambda_1 \cos \Theta & \lambda_2 \sin \Theta & \lambda_1 \rho & -\rho & -\rho \tan \Theta & -\frac{1}{\cos \Theta} \\ -\lambda_2 \cos \Theta & \lambda_2 \sin \Theta & \lambda_2 \rho & -\sin \Theta & \frac{\cos \Theta + \rho^2}{\cos \Theta} & \rho \tan \Theta \end{bmatrix} \quad (19)$$

$$\lambda_1 = A \tan \Theta + B \quad (20)$$

$$\lambda_2 = \frac{A \rho}{\cos \Theta} + C \quad (21)$$

$$(22)$$

$$x \dot{\Theta} \sin \Theta + y \dot{\Theta} \cos \Theta - \dot{\rho} = -\left(\frac{\rho}{\cos \Theta} - y \tan \Theta\right) \quad (23)$$

$$\dot{\Theta} = K_1(p_1, p_0) \cos \Theta v \dot{\rho} = (K_2(p_1, p_2) + K_2(p_1, p_0) \rho \sin \Theta) * v \quad (24)$$

$$\begin{pmatrix} L_\rho^T & L_\Theta^T \end{pmatrix} = \begin{bmatrix} -\lambda_\rho \cos \Theta & -\lambda_\Theta \cos \Theta \\ \lambda_\rho \sin \Theta & \lambda_\Theta \sin \Theta \\ \lambda_\rho \rho & -\lambda_\Theta \rho \\ (1-\rho) \sin \Theta & -\rho \cos \Theta \\ -(1+\rho^2) \cos \Theta & -\rho \sin \Theta \\ 0 & 1 \end{bmatrix} \quad (25)$$

$$\lambda_\rho = -A \cos \Theta + B \rho \sin \Theta + C$$

$$\lambda_\Theta = B \cos \Theta - A \sin \Theta$$

$$L_s = (L_\rho^T, L_\Theta^T)^T$$

II. SERVOING LOOP

We will now show how we can build a command from 2D visual information. To do this, we consider the vector s which represents the measurements extracted from the image. For our case these measurements correspond to the vector $s = (\rho, \Theta)^T$.

We will minimize the error defined by the following relation :

$$e(t) = s - s^* \quad (27)$$

s is the current measure and s^* is the reference measure. We need to determine the relationship between the speed of the visual cues \dot{s} and the velocity of the camera v :

$$\dot{s} = L_s v \quad (28)$$

Where v is a translational speed and rotation vector in 3D $v = (v_x, v_y, v_z, w_x, w_y, w_z)^T$. En utilisant (27) et (28), we obtain the relation between the speed of the camera and the variation in time of the error :

$$\dot{e} = L_s v \quad (29)$$

using the equation (29) we will cancel the error with the introduction of a proportional gain λ

$$v = -\lambda L_s^+ e \quad (30)$$

where L_s^+ is the pseudo-inverse of L_s . continuing the development we find

$$\dot{e} = -\lambda L_s^+ (s - s^*) \quad (31)$$

We close the servoing loop using (29) and assuming that we realize perfectly v

$$\dot{e} = -\lambda L_s L_s^+ e \quad (32)$$

This last equation characterizes the servoing scheme followed. The following relation will make it possible to define the representation of the servoing scheme for four lines .

$$\begin{pmatrix} \dot{\Theta}_1 \\ \dot{\rho}_1 \\ \dot{\Theta}_2 \\ \dot{\rho}_2 \\ \dot{\Theta}_3 \\ \dot{\rho}_3 \\ \dot{\Theta}_4 \\ \dot{\rho}_4 \end{pmatrix} = \begin{pmatrix} L_{\Theta_1} \\ L_{\rho_1} \\ L_{\Theta_2} \\ L_{\rho_2} \\ L_{\Theta_3} \\ L_{\rho_3} \\ L_{\Theta_4} \\ L_{\rho_4} \end{pmatrix} v = L v \quad (33)$$

In this case the use of four lines is justified by obtaining eight equations for the six unknowns of the

velocity of the camera. . The L matrix can be computed in different ways : (1) L_s At the current point s , (2) L_{s^*} at the reference point s^* or (3) $\frac{L_s + L_{s^*}}{2}$ as the center between the first two. The following section compares these three different approaches in terms of convergence.

III. EXPERIMENTAL RESULTS

The visual servoing approach is tested on lines using a free camera (6 degrees of freedom) and four lines. We compare three approaches of visual servoing on lines : (1) An approach that uses the L interaction matrix taken in the current state. (2) An approach that uses the interaction matrix L^* taken at the reference state. (3) An approach that uses the interaction matrix $\frac{L+L^*}{2}$ which is the center of the previous interaction matrices. In the reference state, the camera is aligned with the world marker and at the initialization state the camera is rotated by 5 degrees around its optical axis Z . The focal length of the camera is $f = 1500^1$. We take lines belonging to the plane. $X+Y+Z = 20$. They go through the following points : Line 1 ($[3, 3, 14]$; $[4, 6, 10]$), Line 2 ($[4, 6, 10]$; $[-2, 2, 20]$), Line 3 ($[-2, 2, 20]$; $[-2, -2, 24]$), Line 4 ($[-2, -2, 24]$; $[3, 3, 14]$). For the servoing we take $\lambda = 0.001$ and we put a condition of stopped of the sorvoing when the norm of the differences of visual cues is lower than 0.01. The results are shown in the figures 3, 4, 5. the figure 2 represents the image of the four lines in the initial state with respect to their image in the reference state. From the experiments conducted, it appears that the strategy that uses $\frac{L+L^*}{2}$ as the interaction matrix presents the best results in terms of accuracy and achievement of the state of reference. We note that the speed of convergence is slow (after 2000 iterations). A higher lambda does not allow convergence. We have also noticed that initial states too far from the reference state (more than 10 in rotation and more than 300 mm in translation) do not allow to return to the initial state. . In future work, it would be interesting to study these cases of divergence and to develop a methodology to accelerate convergence even for larger movements.

IV. CONCLUSION

Comparing different four-line visual servoing approaches, we have found that the approach where we use the interaction matrix $\frac{L+L^*}{2}$ which is the center of the interaction matrices at current and reference point provides better results in terms of accuracy and speed of convergence. The use of

1. The units of distances are millimeters and the angles are degrees.

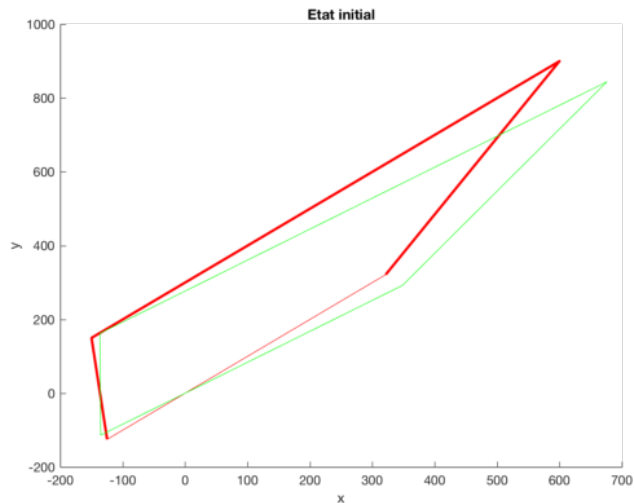


FIGURE 2. Initial state. In red the lines references and in green the lines seen in the initial state.

interaction matrix at one of the two points mentioned above is not recommended in this case. In future works, we will study the different cases of divergences as well as the variations of the singular values of matrices LL^+ which determine the stability of the servo process.

RÉFÉRENCES

- [1] H. Kopka and P. W. Daly, A Guide to L^AT_EX, 3rd ed. Harlow, England : Addison-Wesley, 1999.
- [2] F. Chaumette Image moments : a general and useful set of features for visual servoing ?,*IEEETran s. on Robotics and Automation*,20 (4) :713 -723 , Aug . 2004
- [3] F. Chaumette, S. Hutchinson , Visual servo control Part I : basic approaches ?,*IEEE Robotics and Automation Magazine*, 13 (4) :82 -90 ,Dec . 2006.
- [4] P. Corke, S. Hutchinson ,A new partitioned approach to image-based visual servo control,*IEEETran s. on Robotics and Automation*,17 (4) :507 -515 , Aug . 2001.
- [5] L. Deng , F.Janabi-Sharifi, W.Wil son , ?Hybrid strategies for image constraints avoidance in visual servoing ,*IROS02, Lausanne*, pp 348-353 , Oct. 2002.
- [6] B. Espiau, F. Chaumette, P. Rives, ?A new approach to visual servoing in robotics ?,*IEEETran s.on Robotics and Automation*, 8(3) :313 -326 ,Jun e 1992.
- [7] N. Gans, S.Hutchinson , P.Corke, ?Performance tests for visual servo control systems, with application to partitioned approaches to visual servo control ?,*Int. Journal of Robotics Research*, 22 :955 -981 , Oct.2003.
- [8] N. Gans, S. Hutchinson , ?Stable visual servoing through hybrid switched-systems control,*IEEETran s. on Robotics*, 23 (3) :530 -540 ,Jun e 2007.
- [9] S. Hutchinson , G. Hager, P. Corke, ?A tutorial on visual servo control ? ,*IEEETran s. on Robotics and Automation*, 12 (5) :651 -670 , Oct. 1996.
- [10] F. Janabi-Sharifi, W. Wilson , ?Automatic selection of image features for visual servoing ?,*IEEETran s.on Robotics and Automation* 13 (6) :890 -903 , Dec . 1997.
- [11] E. Mali s, F. Chaumette, S. Boud et, ?2 1/2 D visual servoing ?,*IEEETran s. on Robotics and Automation*, 15 (2) :238 -250 , Apr. 1999.
- [12] E. Mali s, ?Improving vision-based control using efficient second-order minimization techniques ?,*ICRA ?04*, pp 1843-1848, New Orleans, Apr.2004.
- [13] E. Marchand , F. Spindler, F. Chaumette, ?ViSP for visual servoing : a generic software platform with a wide class of robot control skills ?,*IEEE Robotics and Automation Magazine*, vol. 12 (4) :40 -52 , Dec .2005,
- [14] P. Marti net, J. Galli ce , D. Khadraoui, ?Vision based control law using 3d visual features ? ,*Proc.WAC 96*, pp . 497 -502 , Montpellier,May 1996.
- [15] W. Wilson , C. Hull s, G. Bell , ?Relative End Effector Control Using Cartesian Position Based Visual Servoing ? ,*IEEETran s. on Robotics and Automation*, 12 (5) :684 -696 , Oct. 19

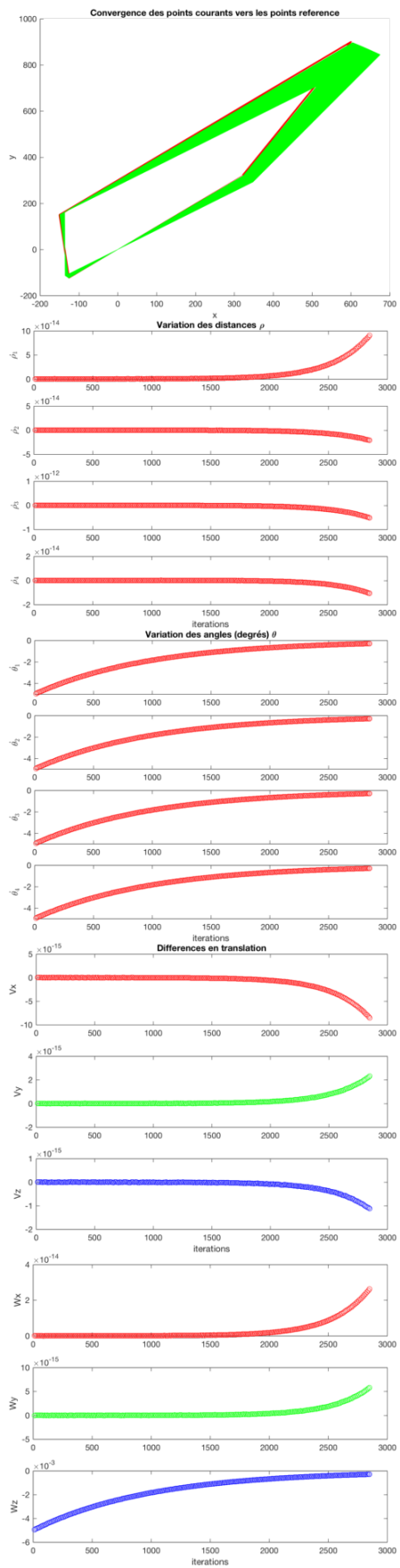


FIGURE 3. Results of the experiment with L .

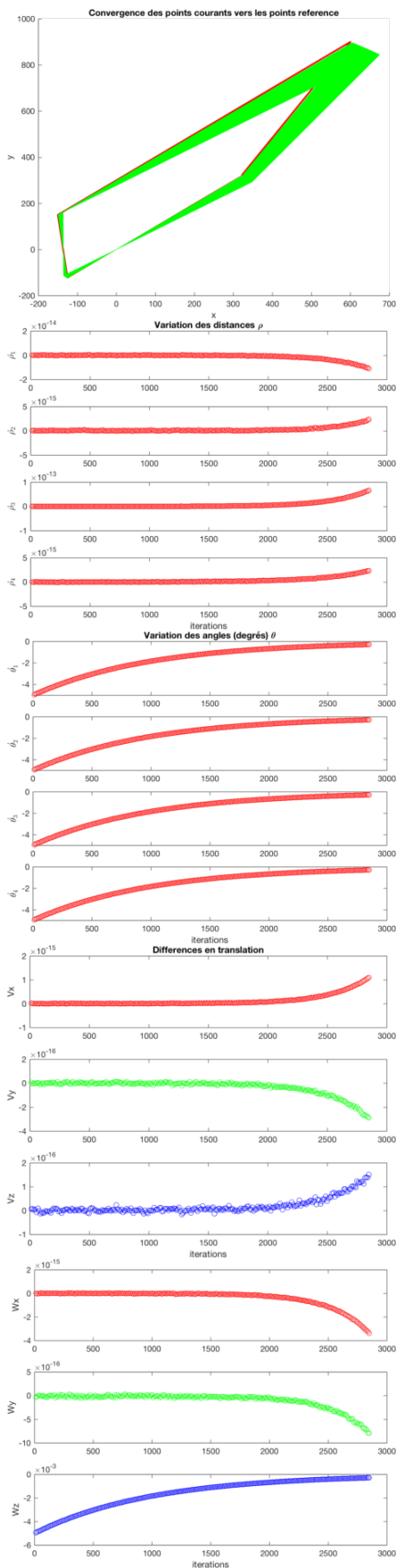


FIGURE 4. Results of the experiment with L^* .

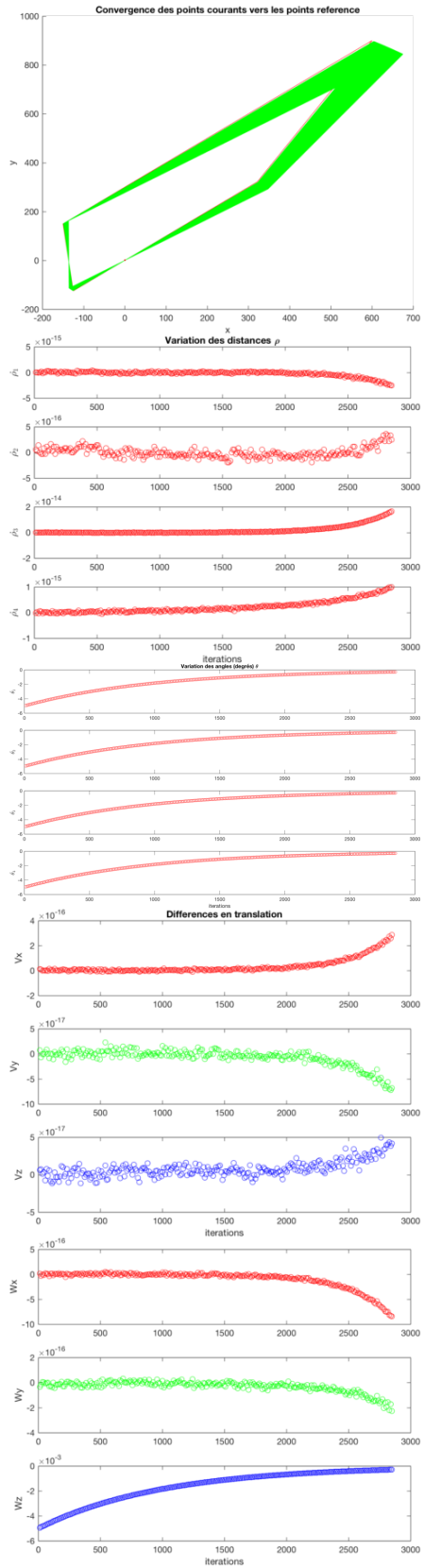


FIGURE 5. Results of the experiment with $\frac{L+L^*}{2}$.